

8-25-2008

Monodomain Alignment of the Smectic-A Liquid Crystalline Phase from the Isotropic Phase

Mitya Reznikov

Kent State University - Kent Campus

Bentley Wall

Kent State University - Kent Campus

Mark A. Handschy

Philip J. Bos

Kent State University - Kent Campus, pbos@kent.edu

Follow this and additional works at: <https://digitalcommons.kent.edu/cpipubs>

 Part of the [Physics Commons](#)

Recommended Citation

Reznikov, Mitya; Wall, Bentley; Handschy, Mark A.; and Bos, Philip J. (2008). Monodomain Alignment of the Smectic-A Liquid Crystalline Phase from the Isotropic Phase. *Journal of Applied Physics* 104(4). doi: 10.1063/1.2969906 Retrieved from <https://digitalcommons.kent.edu/cpipubs/123>

This Article is brought to you for free and open access by the Department of Chemical Physics at Digital Commons @ Kent State University Libraries. It has been accepted for inclusion in Chemical Physics Publications by an authorized administrator of Digital Commons @ Kent State University Libraries. For more information, please contact digitalcommons@kent.edu.

Monodomain alignment of the smectic-A liquid crystalline phase from the isotropic phase

Mitya Reznikov,^{1,a)} Bentley Wall,¹ Mark A. Handschy,² and Philip J. Bos¹

¹Liquid Crystal Institute, Kent State University, Kent, Ohio 44242, USA

²Displaytech, Inc., 2602 Clover Basin Drive, Longmont, Colorado 80503, USA

(Received 11 March 2008; accepted 19 June 2008; published online 25 August 2008)

The liquid crystal alignment method described here provides uniform orientation of otherwise difficult-to-align smectic-A liquid crystal materials lacking a nematic phase. The smectic-A phase is grown in the presence of a 10–20 K/mm temperature gradient from an air bubble located within a cell by a photolithographically defined channel in the cell substrates. We obtain uniform layer alignment in millimeter-wide smectic regions at growth rates below about 0.05 $\mu\text{m/s}$ even though there is a tendency for spontaneous nucleation of focal-conic defects at higher growth rates once the width of the smectic-A region exceeds the critical value of about 20 μm . © 2008 American Institute of Physics. [DOI: 10.1063/1.2969906]

I. INTRODUCTION

The alignment of smectic liquid crystals is of practical interest due to their numerous display applications. Ferroelectric liquid crystal (FLC) displays utilizing chiral smectic-C (SmC*) materials have many attractive features such as fast response time and bistability. Most FLCs used in displays possess an isotropic–nematic–smectic-A (SmA)–smectic-C (I-N-A-C) phase sequence and are usually aligned in their nematic phase using conventional surface-treatment methods such as rubbed polymer surfaces, obliquely deposited SiO_x surfaces, and photoaligned polymer surfaces.

However, there is a class of FLCs with unique characteristics such as large cone angles and reduced layer shrinkage having I-A-C phase sequences. Conventional alignment methods do not work well for these materials due to the absence of the nematic phase. Several methods have been proposed for aligning I-A-C liquid crystals. They include using rubbed nylon as the alignment layer,¹ gentle shearing in the SmA phase,² application of a magnetic field during cooling from isotropic to SmA phase,³ and the spatial-gradient cooling technique,^{4,5} which relies on cooling the liquid crystal from its isotropic phase in the presence of a thermal gradient in the plane of the cell and perpendicular to a nucleating wall. According to this method, as a cell is cooled the SmA-I transition-temperature contour line moves parallel to the nucleating wall and out into the liquid crystal to grow a band of smectic phase out from the wall. The use of this technique and I-A-C materials has the advantage, as suggested by Ishikawa *et al.*,⁴ that the cell surface treatment can be chosen for its effect on the director in the smectic phase of interest without regard to how it aligns a nematic liquid crystal. For example, as we will show in another paper, it is possible to make a smectic-C* device with bookshelf layer geometry on surfaces that promote homeotropic director alignment.

The gradient cooling technique has proven to be useful;

however in the discussed case where the director aligns parallel to the nucleation wall, the alignment of the smectic layers is often imperfect. Perhaps improved layer alignment could be achieved if the layers were aligned parallel to the nucleating wall and perpendicular to the applied gradient, as in this case where the nucleation wall will tend to promote smectic ordering and the gradient direction is along a symmetry direction of the layered structure. While the use of walls that promote homeotropic alignment of the director (parallel alignment⁵ of the smectic layers) has been previously proposed⁵ it has not yet been demonstrated. On the other hand, growth of SmA monodomains from air bubbles was reported for I-N-A-C materials,⁶ and it was shown that smectic layer orientation was not influenced by the surface anchoring.

In this paper we demonstrate a spatial-gradient cooling alignment technique that utilizes an air bubble as the nucleating wall. Along with the advantages of this technique we discuss the problems found in applying this method and their solutions.

II. EXPERIMENT

We initially tried growing smectic layers from nucleating walls made of polymers selected to promote homeotropic alignment but never achieved good results. However, we noticed homeotropic alignment around air bubbles in the cell. To explore the use of bubbles as the nucleating wall we constructed an experimental setup where an elongated air bubble, defined and contained by a lithographically etched channel in the cell substrate, is aligned normal to a temperature gradient in the plane of the cell, as shown in Fig. 1. Channels were etched into an indium tin oxide (ITO)-coated glass using a photopatterned resist and hydrofluoric acid. Upon completion of the photolithography process, the substrates were thoroughly washed and the surface treatment, if any, was deposited.

To investigate the effect, or lack of effect, of surface treatments on the smectic layer alignment, we made cells with each of the following: clean ITO, SiO_x deposited at 5°

^{a)}Author to whom correspondence should be addressed. Electronic mail: mitya@lci.kent.edu.

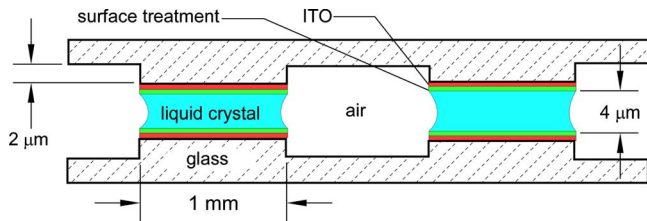


FIG. 1. (Color online) Design of liquid crystal cell (not drawn to scale). Channel substrates were made by photolithographic etching of standard ITO-coated glass with hydrofluoric acid.

(85° incidence angle to surface normal), SiO_x deposited at 30°, Glymo (3-glycidoxypropyltrimethoxysilane), Nissan 7511 and 1211 polyimides, and Dupont PI-2555 polyimide. When assembling the cell, it is possible to use two substrates with channels, as shown in Fig. 1, or one substrate with channels and one plain ITO substrate. While it may be expected that the first case will yield a more symmetric air-liquid crystal interface, we found that in most cases the simpler second case also works well. The cell gap was defined by powder spacers that were mixed in the UV-sensitive glue, which held two substrates together. We measured the empty cell gap using the optical interference method. For most of our alignment experiments the cell gap was about 4 μm , although some experiments were done with thinner cells (cell gap of about 1.5 μm). The cells were filled with liquid crystals in isotropic phase using the capillary filling method so that only the spaces between the channels were filled with liquid crystal, leaving the channels to contain only air. To prevent the liquid crystal from filling air channels, we limited the amount of the liquid crystal. We used the following liquid crystal materials, all without nematic phase: 10CB (I-51°C-SmA), 12-S5 (4'-pentylbenzenethiol-4-dodecyloxybenzoate: I-90°C-SmA-87°C-SmC-60°C-K), and Displaytech MX10498 (I-95°C-SmA-86°C-SmC-30°C-K). All gave similar results in our experiments. A rough drawing of the thermal gradient setup is shown in Fig. 2. The liquid crystal cell was placed between four metal plates (two at each side) to direct a thermal gradient across the channels. The distance between the plates was about 6 mm. We used ceramic heating elements and a refrigerated circulating water bath, both with thermocouple sensors and under computer control, to set the temperatures of the hot side and cold side, respectively. Thermocouple sensors were tightly secured between metal plates (schematically shown in Fig. 2) to ensure good thermal contact. We put this setup on the stage of a polarizing microscope to observe the alignment process.

With the cell between the plates we set the temperature of both sides so that the whole sample would become isotropic and then started slowly cooling the cold side. The ther-

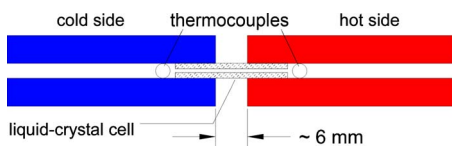


FIG. 2. (Color online) Scheme of gradient heater. Liquid crystal cell is placed between cooled and heated metal plate elements to create a spatial thermal gradient along the cell.

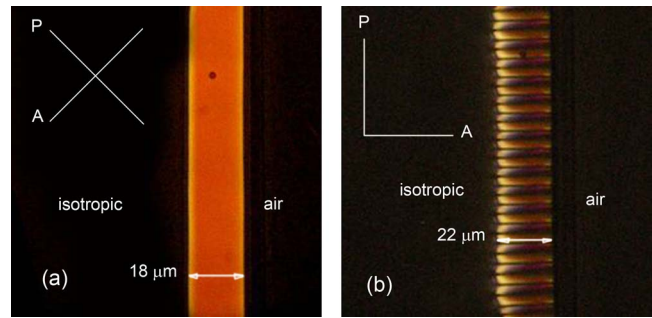


FIG. 3. (Color online) Growth of SmA band from air bubble wall: (a) uniformly aligned band below critical width; (b) band with defect structure above critical width. Displaytech MX 10498 on alignment layer of Nissan 7511 polyimide in this and further photographs, unless otherwise noted.

mal gradient when the cold side was cooled sufficiently to cause the SmA-I transition line to be at the spatial location of the air/liquid crystal interface was approximately 10 K/mm. As we continued to cool the cold side, the thermal gradient value gradually increased to about 20 K/mm when the SmA-I transition line moved across the area of the liquid crystal to be aligned. Depending on the temperature phase transitions of the liquid crystal, a steep thermal gradient sometimes resulted in the coexistence of more than one liquid crystalline phase over a 1 mm area (usually SmA and SmC), which, however, did not disturb the alignment process.

Initially we observed a monodomain, defect-free SmA layer nucleating and growing from the air/liquid crystal interface, as shown in Fig. 3(a). The dark area to the right of the bright stripe of the SmA band contains air, while the dark area to the left of the stripe contains isotropic liquid crystal. However, when the smectic stripe reached a particular width we observed a dramatic structural change as can be seen in Fig. 3(b). The typical value of this threshold width was about 20 μm . Before this change smectic molecules were uniformly aligned normal to the nucleation edge. In Fig. 3(a) this structure is shown with nucleation edge at 45° to the crossed polarizer and analyzer. Had the polarizer been parallel to the nucleation edge the smectic monodomain would have appeared dark and undistinguishable from the background. After the structural transition the smectic phase has the appearance shown in Fig. 3(b).

After further cooling to allow the width of the SmA stripe to grow, it acquires the appearance shown in Fig. 4(a). Surprisingly, the effect of the defects at the SmA-I interface

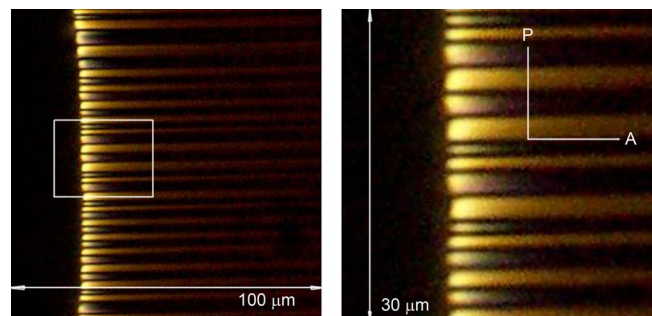


FIG. 4. (Color online) SmA-I interface after further cooling.

has weakened and a nearly uniform texture is seen along the right (cooler temperature) side of the smectic band. We initially thought that the structural transition apparent in Fig. 3(b) would prevent attainment of uniform alignment over wider bands, but we subsequently found that with extremely slow cooling rates, good alignment could be obtained due to the annealing effect seen in Fig. 4. At the onset of cooling, before the smectic stripe reached its critical thickness, as shown in Fig. 3(a), the cooling rate can be relatively high. Uniform smectic layers grew as a monodomain as long as the cooling rate was lower than 1 K in 2 min. However, after the structural transition the critical cooling speed had to be less than around 1 K per 20 min, corresponding to a growth rate of the smectic band at about $0.05 \mu\text{m/s}$. Faster cooling rates typically produced a cascade of defects, with appearance depending on the cooling rate, as can be seen in Fig. 5. If the cooling rate produced growth of the smectic band exceeding our very slow rate at about $0.05 \mu\text{m/s}$, elongated bâtonnets start to “shoot out” from the interface, as can be seen in Fig. 5(a). Further cooling-rate increase to produce smectic-band growth of around $0.1 \mu\text{m/s}$ caused bâtonnets to form in the isotropic phase close to the interface, as can be seen in Fig. 5(b). Such defects disrupt the monodomain alignment, as can be seen in Fig. 6(a), but they can be removed by heating the sample a little to the point where the defects melt and then resuming cooling, with results shown in Fig. 6(b). With low cooling rates we found it possible to grow a fully aligned 1-mm-wide monodomain, as shown in Fig. 7. Although our channel pattern limited the width of the smectic band to 1 mm, it is clear that this method using an air interface for layer nucleation, a high thermal gradient, and a very slow cooling rate could be used to obtain arbitrarily large SmA domains.

Figure 8 shows the results of alignment obtained on different surfaces. In Figs. 8(a) and 8(c), the texture of Displaytech MX10498 is shown; in Fig. 8(b), the liquid crystal is 12-S5. These pictures have different colors due to variation in the cell gaps and difference in the liquid crystalline material birefringence. Using alignment layers of Glymo, 5°SiO_x , and 30°SiO_x gave very similar results. We present them here to show that the quality of the SmA layer alignment was not influenced by the choice of cell-substrate surface treatment. We obtained good alignment with all the surface treatments we tried. The quality of alignment did not depend much on the surface layer but rather on experimental conditions related to the temperature profile in the cell. We found that the alignment quality was very sensitive to temperature fluctuations, such as those of the heater and cooler, or even of air movements near the cell. The value of the temperature gradient was also very important to obtain monodomain alignment. A high gradient was required to stabilize the SmA-I interface and to prevent bâtonnets from forming ahead of the interface. When the gradient was not steep enough focal conics tended to nucleate on the interface, disrupting the monodomain. We found that thermal gradients of 10–20 K/mm were sufficient.

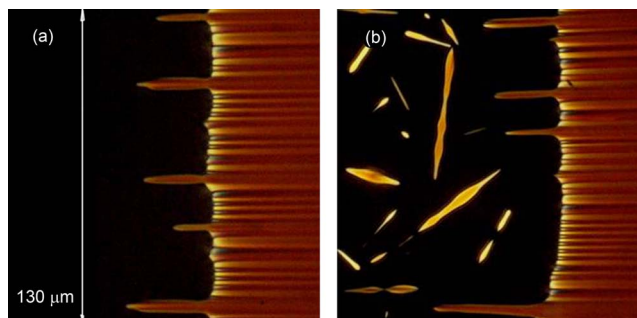


FIG. 5. (Color online) Alignment defects appearing at different growth rates: (a) $0.1 \mu\text{m/s}$; (b) $0.2 \mu\text{m/s}$.

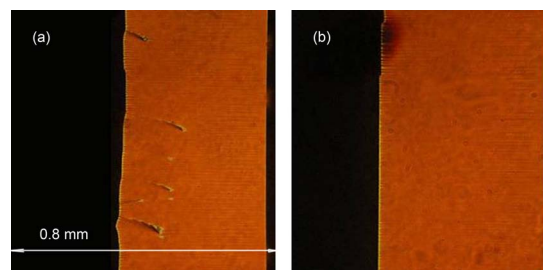


FIG. 6. (Color online) Annealing of defects formed in SmA: (a) initial appearance after nucleation of defects; (b) appearance after melting and cooling again—defects disappeared.

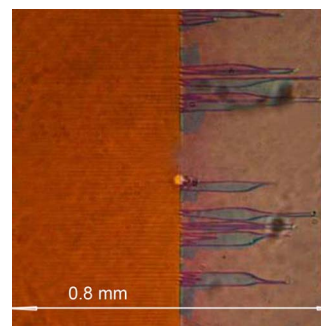


FIG. 7. (Color online) Uniform alignment across full smectic band width. Due to thermal gradient the left side of the picture is in the SmA phase and the right side is in the SmC phase.

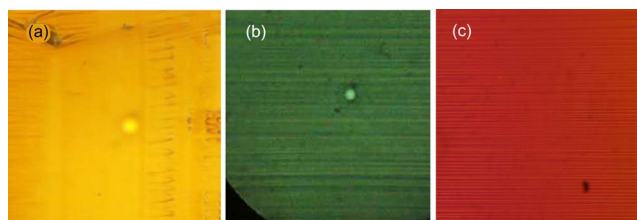


FIG. 8. (Color online) Alignment results on different surfaces: (a) Dupont polyimide 2555, (b) clean ITO, and (c) Nissan polyimide 1211. Crossed polarizers are at 45° with respect to the layer normal.

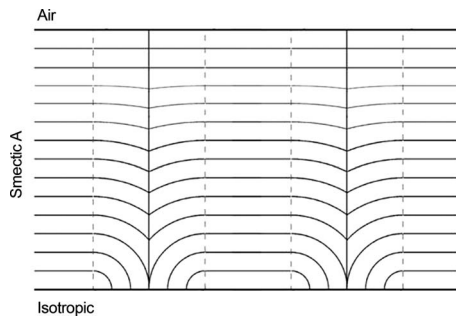


FIG. 9. Proposed structure SmA layers at onset of defect formation.

III. DISCUSSION

The method described above nucleates smectic layers parallel to a molecularly smooth interface formed by an air bubble in the liquid crystal. The main difficulty in obtaining uniform large-area alignment with this method arises from focal-conic defects that spontaneously appear at the SmA/isotropic interface after the width of the smectic band exceeds some critical value, similar to a phenomenon previously observed by Fournier *et al.*⁷ Fournier *et al.*⁷ considered a SmA liquid crystal sample floating on an isotropic droplet, with a temperature gradient across the thickness of the sample. They pointed out that at the air/SmA interface the smectic layers prefer to align parallel to the interface (liquid crystal molecules are aligned homeotropically at the interface), while at the SmA/isotropic interface the layers tend to align perpendicularly to the interface (planar alignment of the liquid crystal molecules). These antagonistic boundary conditions produce texture distortions, involving both layer dilation and curvature,⁷ which, in turn, lead to the appearance of focal-conic defects at the interface, as observed for the first time in 1910 by Friedel and Grandjean,⁸ as well as in more recent works.^{7,9} We conclude that the smectic band in our experiments has a structure similar to that shown in Fig. 8. However, we have observed under the polarizing microscope that some regions never appear dark between crossed polarizers regardless of the sample orientation with respect to the polarizers' axis, implying some twisting of the layer structure through the thickness of the cell and that the exact layer configuration may be more complex than shown in Fig. 9. Subsequent study by Fournier *et al.*¹⁰ of the growth dynamics of the smectic slab found that a critical growth rate for their system was about $25 \mu\text{m/s}$, above which growth instabilities of the SmA/isotropic interface led to nucleation of focal-conic domains. In an analogy with the Mullins–Sekerka¹¹ instability, where growth velocity was limited by the diffusion of impurities, they estimated a threshold cooling rate of $50 \mu\text{m/s}$, in good agreement with their experimental results.

We found that once defects begin to cascade, as shown in Fig. 5, it was not possible to continue the growth of a uniformly aligned SmA domain. However, our experiments show that if the cooling rate is drastically decreased to about $0.05 \mu\text{m/s}$, a uniform layer formation is possible even in smectic bands thicker than the threshold thickness for defect formation. We suggest that at growth rates low enough that the distorted focal-conic structure can relax to a uniform un-

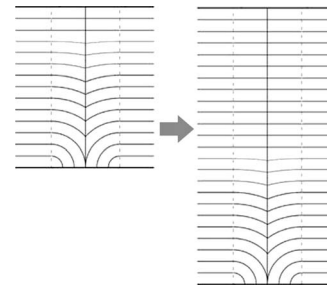


FIG. 10. Annealing from focal-conic distorted structure to uniform undistorted structure during slow cooling.

distorted one, flat smectic layers continue to form, as depicted in Fig. 10. In their study of the focal-conic structure of SmA bâtonnets, Fournier and Durand¹² argued that permeative flow in the SmA phase increased the persistence of structural irregularities they called *sailles* to times on the order of 0.3 h, consistent with our finding that a very slow cooling is required in order for defects to anneal away.

IV. CONCLUSIONS

We have demonstrated an alignment method that does not rely on surface treatments for aligning liquid crystal materials that have a SmA/isotropic phase transition. It uses an air bubble, located by a photolithographically defined channel, to create a smooth wall for nucleation of smectic layers and to induce perpendicular molecular orientation for liquid crystal molecules. However, antagonistic boundary conditions lead to nucleation of focal-conic defects in the growing SmA region once it attains a threshold size of a few tens of microns. These focal-conic defects persist unless the SmA is grown in the presence of a large temperature gradient and at a cooling rate slow enough that the SmA growth velocity is low ($\sim 0.05 \mu\text{m/s}$), in which case the focal-conic regions anneal to a uniform structure. We obtained a very good quality of smectic layer alignment over large areas regardless of a variety of different surface treatments. Future use of more-localized heating, such as could be provided by a scanned laser, will allow the whole cell to be maintained at a temperature close to the SmA-I transition temperature with only a thin line heated to the isotropic phase. This should decrease the focal-conic relaxation time, allow faster motion of the interface line, and make the alignment method more convenient for industrial applications.

ACKNOWLEDGMENTS

This material is based on work supported by the United States Air Force under Contract No. FA9453-04-C-0163.

¹D. Williams and L. E. Davis, *J. Phys. D* **19**, L34 (1986).

²N. A. Clark and S. T. Lagerwall, *Appl. Phys. Lett.* **36**, 899 (1980).

³K. Kondo, Y. Sato, K. Miyasato, H. Takezoe, A. Fukuda, E. Kuze, K. Flatischler, and K. Sarp, *Jpn. J. Appl. Phys., Part 2* **22**, L13 (1983).

⁴K. Ishikawa, K. Hashimoto, H. Takezoe, A. Fukuda, and E. Kuze, *Jpn. J. Appl. Phys., Part 2* **23**, L211 (1984).

⁵K. Kondo, H. Takezoe, A. Fukuda, and E. Kuze, *Jpn. J. Appl. Phys., Part 2* **22**, L85 (1983).

⁶I. Dozov and G. Durand, *Europhys. Lett.* **28**, 25 (1994).

⁷J. B. Fournier, I. Dozov, and G. Durand, *Phys. Rev. A* **41**, 2252 (1990).

⁸G. Friedel and F. Grandjean, *Bull. Soc. Fr. Mineral.* **33**, 409 (1910).

⁹J. Michel, E. Lacaze, M. Alba, M. de Boissieu, M. Gailhanou, and M. Goldmann, *Phys. Rev. E* **70**, 011709 (2004).

¹⁰J. B. Fournier, M. Warengem, and G. Durand, *Phys. Rev. E* **47**, 1144 (1993).

¹¹W. Mullins and R. Sekerka, *J. Appl. Phys.* **35**, 444 (1964).

¹²J. B. Fournier and G. Durand, *J. Phys. II* **1**, 845 (1991).